

# Manifestations of Degassing in Sedimentary Cover of the Southeastern Flank of the Knipovich Ridge (North Atlantic)

S. Yu. Sokolov<sup>a, \*</sup>, G. D. Agranov<sup>a, b</sup>, S. I. Shkarubo<sup>c</sup>, A. V. Zayonchek<sup>a</sup>, and A. S. Abramova<sup>a</sup>

<sup>a</sup> *Geological Institute, Russian Academy of Sciences, Moscow, 119017 Russia*

<sup>b</sup> *Earth Sciences Museum, Lomonosov Moscow State University, Moscow, 119991 Russia*

<sup>c</sup> *JSC Marine Arctic Geological Expedition, Murmansk, 183038 Russia*

\**e-mail: sysokolov@yandex.ru*

Received January 18, 2022; revised February 18, 2022; accepted April 29, 2022

**Abstract**—The paper analyzes the “bright spot” and “flat spot” anomalies of seismic data on the southeastern flank of the Knipovich Ridge associated with the accumulation of free gas in the sedimentary cover above the oceanic basement. The identified anomalies are associated spatially with negative values of the residual Bouguer anomaly and positive magnetic field ( $\Delta T_a$ ) anomalies. This fact indicates the existence of decompaction zones in the crust and upper mantle related to serpentinization that can also provoke the superimposed, probably modern, chemogenic magnetization and distortion of the primary linear pattern of magnetic anomalies in the oceanic basement in the study area. Serpentinization was also responsible for vertical displacements of the crustal and upper mantle blocks on the flanks, leading to deformations of the sedimentary cover with the rock dilation. Off-axis seismicity indicates tectonic disruptions on flanks of the ridge with a higher access of water necessary for the serpentinization and the subsequent change in the physical properties of rocks reflected in geophysical fields. The eastern flank of the Knipovich Ridge underwent tectonic activation along the basement structures representing the northern extension of the Senja fracture zone, resulting in accumulations of free gas in the sedimentary cover.

**Keywords:** Knipovich Ridge, gas pools, serpentinization, “bright spot” seismic anomalies, Bouguer anomaly, anomalous magnetic field

**DOI:** 10.1134/S0024490222050078

## INTRODUCTION

Seismic studies of the sedimentary cover on flanks of the Knipovich Ridge (Fig. 1) provided insight into the distribution of its thickness on the spreading basement in small-scale (Straume et al., 2019) and large-scale models (Shkarubo, 1996; Yampolsky and Sokolov, 2012), tectonic structure (Amundsen et al., 2011; Kvarven et al., 2014; Peive and Chamov, 2008; Shipilov et al., 2006; Zayonchek et al., 2010) and to accomplish seismostratigraphic subdivision (Amundsen et al., 2011; Chamov et al., 2010; Kvarven et al., 2014; Zayonchek et al., 2010). Previous researchers did not pay much attention in studying the seismo-facies features of sediments and their differences on the western and eastern flanks. Nevertheless, facies studies were carried out for the contourites in connection with the circulation of bottom waters along the continental slope west of Spitsbergen (Svalbard) (Rebesco et al., 2013, 2014) and sedimentary sequences of the Vestnesa Ridge with manifestations of degassing and pseudobottom reflectors defined as bottom simulated reflectors (BSR), which represent the bottom of the gas hydrate layer (Plaza-Faverola and Keiding, 2019),

and the Svyatogor Rise (Johnson et al., 2015; Waghorn et al., 2018). Degassing on the bottom surface is manifested as holes on the bottom (pockmarks remaining after gas emissions) and zones of bubble discharge into the water column. In the sedimentary sequence, free gas pools appear in seismic sections as bright spots related to a drastic increase in the reflected wave amplitude due to an increased contrast of the acoustic properties of the host medium and gas-saturated layers. Sometimes, the free gas dramatically enhances the signal scattering, leading to a sharp attenuation of reflections from the underlying sequences. If gas pools under a local or regional fluid-confining bed (quite often, BSR), are quite large, the impermeable bed is underlain by a sufficiently thick layer exceeding the resolution of the applied reflected wave method. In this case, the lower edge of the gas saturation zone acquires a flat shape, and the reflection from it is called “flat spot” if the amplitude contrast is retained. In the of the Knipovich Ridge area, in addition to the Svyatogor Rise, bright spots were detected on the eastern flank at 76°25' N (Rajan et al., 2012) in a seismic section studied by the refracted wave method. The obtained boundary velocity values suggest that the

upper mantle located under the detected bright spot represents an area of serpentinization provoked by the contact of mantle rocks with seawater and the consequent formation of hydrogen and methane. The seismic data used in this article are related to the manifestations of anomalies of the “bright” and “flat” spot types. In this paper, we studied this phenomenon by mapping the spatial distribution of bright spots and comparing their morphometric characteristics with geophysical fields that reflect the metamorphism of upper mantle rocks during serpentinization. The aim of these studies is to determine the possible tectonic nature of basement structures, which are overlain by bright and flat spots in the sedimentary cover, and to reconstruct their and the gas pool distribution pattern in sedimentary sequences.

### STRUCTURE OF THE BASEMENT AND ORIGIN OF FLUIDS

The structure of the oceanic basement of the Knipovich Ridge and its flanks is shown on the tectonic scheme (Shkarubo, 1996). This is the only open access work showing the structural surface of the basement in the southeastern ridge edge by isohypses. The “continental” area of the Barents shelf subplatform (in east) and the area of the newly formed spreading oceanic crust (in west) are separated by the continent–ocean transition region, where the continental crust was subjected to intense destruction. Of particular interest is tracking of the destroyed continental–newly formed oceanic crust contact zone, which reflects the onset of the ocean floor spreading. In plan view, it is a stepped boundary. Such “spreading” crust boundary, consisting of shear and normal fault segments, was previously established in the northern Atka trough (Baturin, 1993). In the south, this zone coincides with the Senja regional fault: from 74° N to Cape Serkap, it stretches along 13°–14° E, further to the north it gradually shifts westward to the Molloy fracture zone (Fig. 2).

According to the anomalous magnetic field ( $\Delta T_a$ ) data (Mosar et al., 2002; Sokolov, 2011), direction of the basement spreading of the Knipovich Ridge flanks inherited the trend set by the orientation of segments of the initial continental crust breakup (Baturin, 1993), with the subsequent reorientation by ~45° during the spreading axis jump to its current W–E position. In accordance with the interpretation of seismic data and the latest results of aeromagnetometric studies (Gernigon et al., 2020), the initial disclosure of the Norwegian–Greenland Basin section with the future Knipovich Ridge began along the ocean–continent transform boundaries in the Senja and Hornsund fracture zones in a rotation-shaped pattern with the center located in the southwestern Mohns Ridge about ~260 km north of Jan Mayen Island. At present, the basement at the NNE extension of the Senja fracture zone accommodates structures with a similar orientation but not coinciding with azimuths of the main tec-

tonic elements in the modern spreading zone—at segments and transform displacements. Seismic activity of the eastern flank of the Knipovich Ridge (Sokolov et al., 2017) indicates tectonic activation in this part of the basin along the continuation of the Senja fracture zone (Fig. 3). The development of long-lived displacement planes during the prevailing extension creates ideal conditions for the penetration of seawater into the upper mantle, resulting in the serpentinization with the release of hydrogen and methane.

Studies in 1970–1980, carried out in places of the World Ocean with outcrops of ultrabasic mantle rocks, revealed several orders of magnitude higher  $\text{CH}_4$  concentration relative to the background value (Bougault, 2012; Charlou et al., 1998; Dmitriev et al., 1999; Keir et al., 2005). At the same time, the isotopic composition ( $\delta^{13}\text{C}$ ) clearly indicated the abiogenic origin of hydrocarbon. These authors assumed the  $\text{CH}_4$  formation by geochemical processes. Access of water to ultrabasic rocks in the upper mantle through a fracture system promotes the serpentinization at a temperature ranging from ~100° to ~450° C (and, probably, higher). In this process, serpentine and magnetite are formed from olivine. In addition,  $\text{H}_2$  is released to interact with  $\text{CO}_2$  dissolved in water, resulting in the formation of  $\text{CH}_4$ . Upon entering the water,  $\text{CH}_4$  makes up abnormal concentrations in the water column. If the sedimentary cover is developed at fluid seepages from the crystalline crust, the gas is retained in sediments, resulting in the formation of seismic records typical of the gas-saturated media.

The most favorable situation for this process is found where the oceanic crust, formed during the slow and ultra-slow spreading, contains minimal basalt and gabbroid layers along with a sedimentary cover capable of retaining the fluid. If such sediments are lacking,  $\text{CH}_4$  falls directly into the water column, as was established along the eastern wall of the Knipovich Ridge (Cherkashev et al., 2001). The realization of such conditions was studied on the eastern flank of the Knipovich Ridge (Rajan et al., 2012), where the upper mantle is complicated by deep detachment zones with reduced seismic velocities (Kandilarov et al., 2010) and the sedimentary cover (two-way traveltimes up to 2.5 s) included seismic record anomalies typical of the presence of fluids.

In addition to the formation of fluids (Dmitriev et al., 1999), serpentinization is accompanied by the appearance of a new magnetoactive layer due to the formation of magnetite, dilatation of the rock subjected to serpentinization, and simultaneous decrease of its density down to 20% (*Fizicheskie ...*, 1984), as well as manifold increase heat flow due to the exothermic effect of this process (Delescluse and Chamot-Rooke, 2008). The formation of chemogenic magnetite undoubtedly affects the primary linear image of magnetic anomalies by imposing an additional component that creates a mosaic pattern of the anomalous mag-

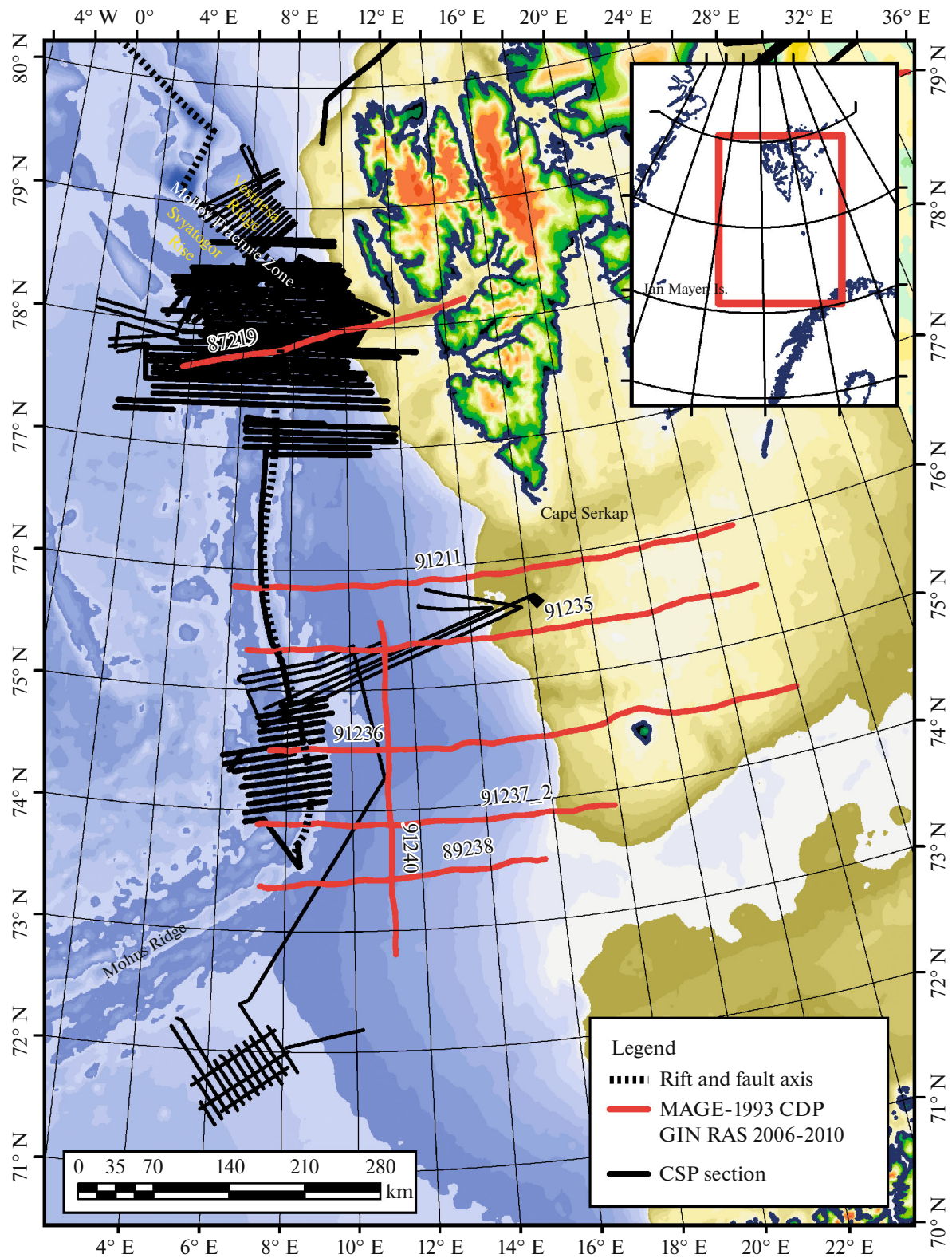


**Fig. 1.** Scheme of study by the CDP seismic reflection method (CDP-SRM), multibeam echosounding, and continuous seismic profiling (CSP) of the Knipovich Ridge area, based on the data of Marine Arctic Geological Expedition (1993) and Geological Institute, Russian Academy of Sciences (Cruises 24–27 of the R/V *Akademik Nikolaj Strakhov*, 2006–2010).

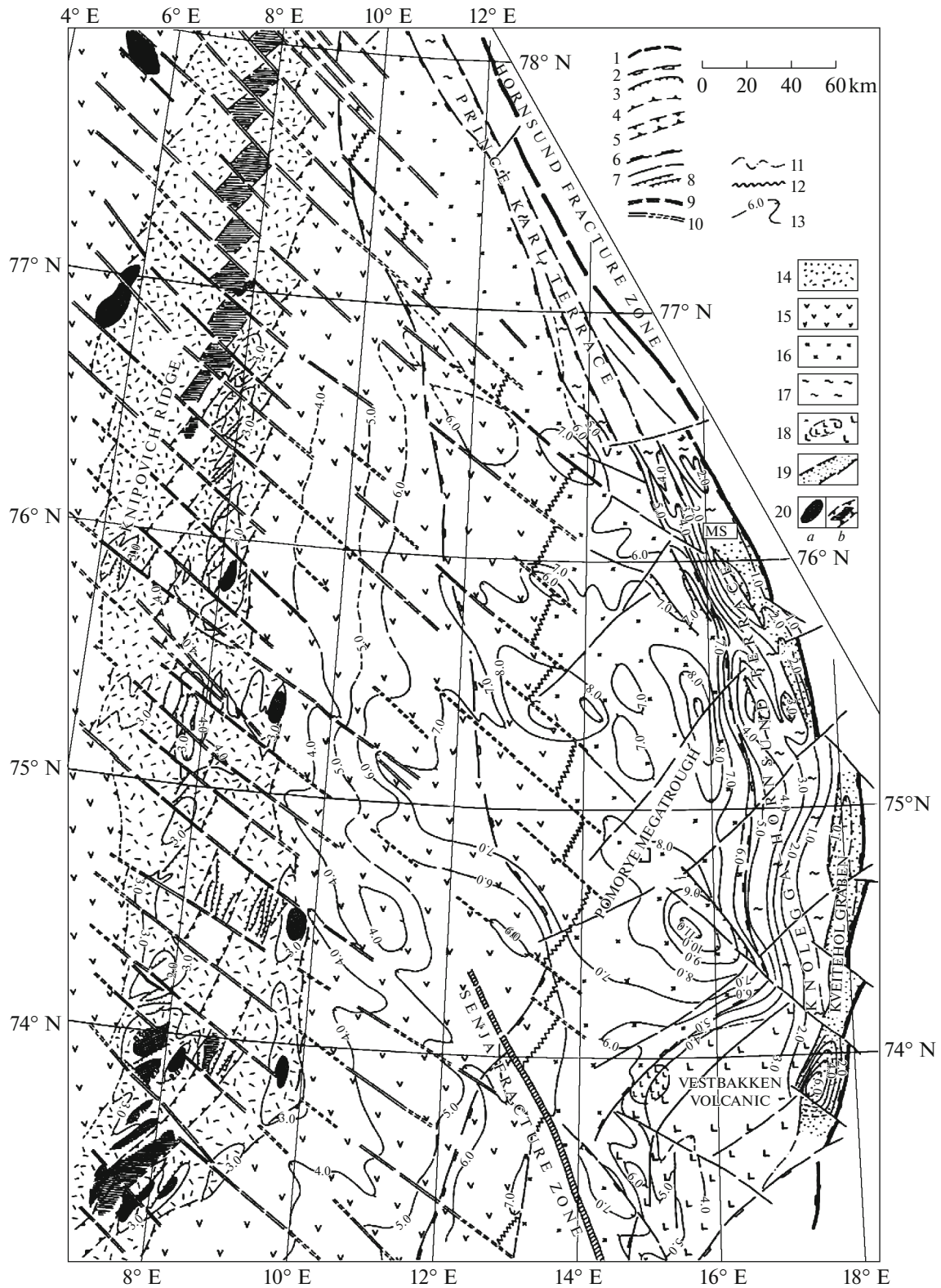


**Fig. 2.** Tectonic scheme of the northeastern Norwegian–Greenland Basin, according to (Shkarubo, 1996). (1–5) Boundaries of structures: (1) Barents subplatform, (2) Medvezhye–Spitsbergen (MS) terrace and Pomorye megatrough, (3) shelf grabens, (4) Knipovich Ridge crest, (5) axial rift; (6–10) fracture zones: (6) Knolegga–Hornsund boundary fracture zone, (7) major normal and transverse faults, (8) local normal faults, (9) largest transform fault zones, (10) transform faults in the median ridge; (11) boundary of the trap field in the Vestbakken province; (12) the assumed boundary of the spreading oceanic crust; (13) isohypses of the basalt basement surface; (14–20) lithostructural sequences and tectonic zones of the transition region and oceanic basin: (14) neotectonic crest of the Knipovich Ridge with a thin layer of dislocated Neogene–Quaternary sediments, (15) Cenozoic sedimentary (nondislocated) sequences on the oceanic crust, (16) Cenozoic sedimentary sequences on the transitional crust, (17) the same, on the continental substrate, (18) field of the Eocene volcanic sedimentary cover (Vestbakken province), (19) shelf grabens with the Paleogene–Early Neogene infill, (20) outcrops of the basalt basement on the ocean floor surface: (a) volcano-tectonic ridges in the range; (b) outcrops of the rift valley.

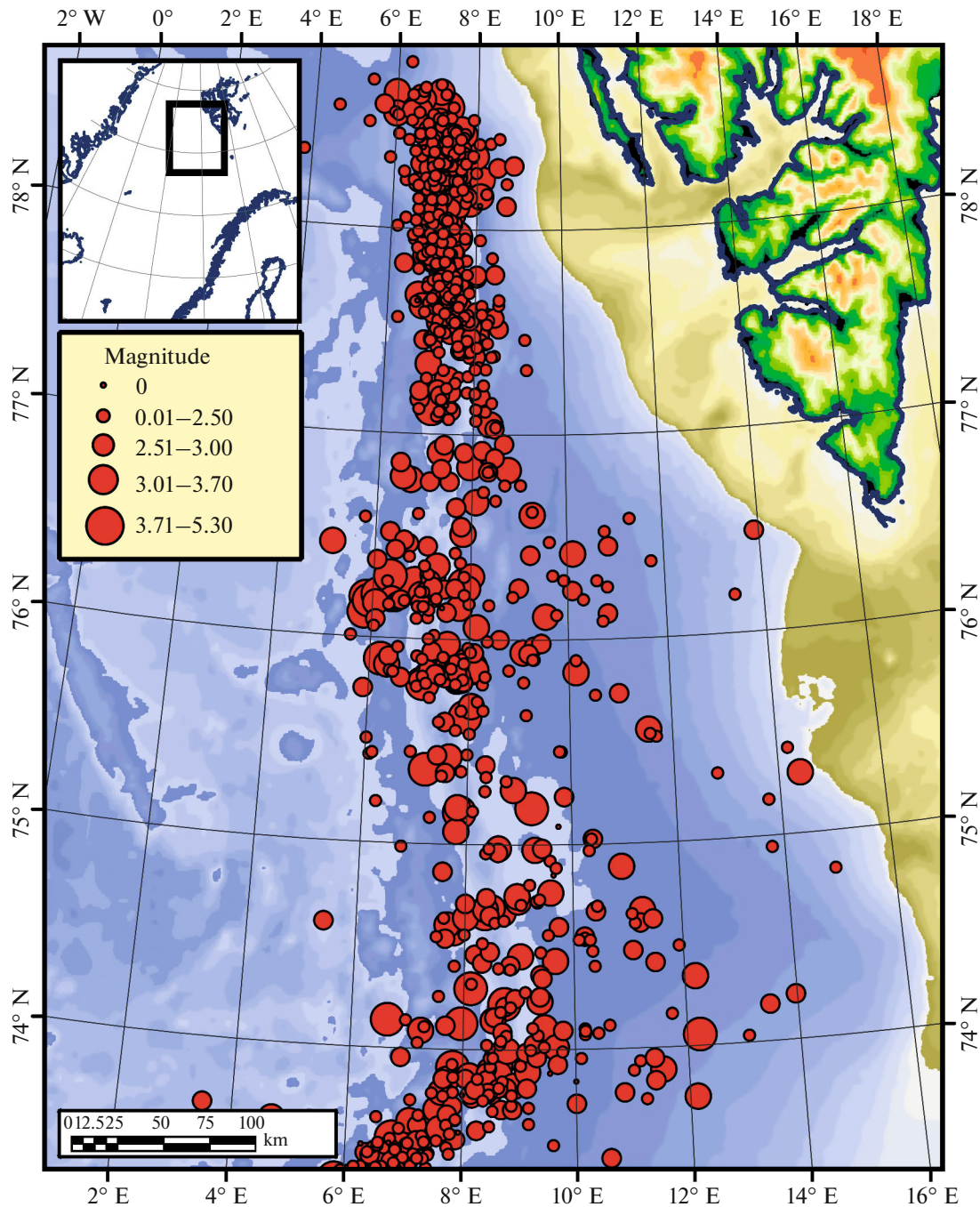


**Fig. 3.** Earthquake epicenters, based on (NORSAR, 2012) in the Knipovich Ridge area.

netic field in the study area (Olesen et al., 1997), where it is very difficult to differentiate the primary and superimposed components of the field. Decompression caused by the serpentinization and the consequent rock dilation can be quite responsible for the positive vertical movements in the crustal crystalline blocks, the formation of a fault network, deformations in the sedimentary cover, and the formation of conduits for fluid migration upward the section.

The seismostratigraphic differentiation of the sedimentary cover on the eastern flank of the Knipovich Ridge has a specific feature associated with thick Quaternary alluvial fans. According to (Amundsen et al., 2011), the cover consists of glacial and preglacial sequences. The preglacial sequence is restricted at the bottom by an acoustic basement composed of a spreading magmatic layer of the oceanic crust. The age of sediments overlying the basement varies from the Eocene in east to the Pliocene in west. The glacial sequence, composed of three Quaternary subsequences, is separated by seven reference reflectors extending from the shelf edge to the rift valley wall of the Knipovich Ridge. The section presented in (Amundsen et al., 2011) has a glacial sequence up to 1 km thick. Total thickness of sediments on the eastern side of the Knipovich Ridge on the oceanic substrate can reach ~6000 m (Straume et al., 2019), and average thickness is ~3500 m. Gas pools making up the bright and flat spots are found in both sedimentary sequences.

#### ANALYTICAL DATA

This work is based on unpublished materials in the Russian Federal Geological Fund (RFGF) and the digital data based on the common depth point technique of seismic reflection method (CDP-SRM) (Fig. 1). The materials were obtained by Marine Arctic Geological Expedition (MAGE) in 1989–1992 on the Barents Sea shelf and the western continental slope up to the Knipovich Ridge. The continuous seismic profiling (NSP) data obtained by the Geological Institute, Russian Academy of Sciences, in cruises 24, 25, 26, and 27 of the R/V *Akademik Nikolaj Strakhov* (2006–2010) were also used. In addition, we used open access data on the gravity field and its reductions (Balmino et al., 2012), as well as the anomalous magnetic field (Maus et al., 2009) compiled within  $[2' \times 2']$  grids.

#### DATA PROCESSING METHODS

The summarized CDP-SRM time sections were loaded into the RadExPro software package for interpreting the seismic data with the picking of bright and flat spots as a discrete horizon beyond the stratigraphic reference. We also included the single-channel CSP sections with picking of the above-mentioned seismic anomalies. Due to a significantly lesser depth of the CSP sections, the spots were identified exclu-

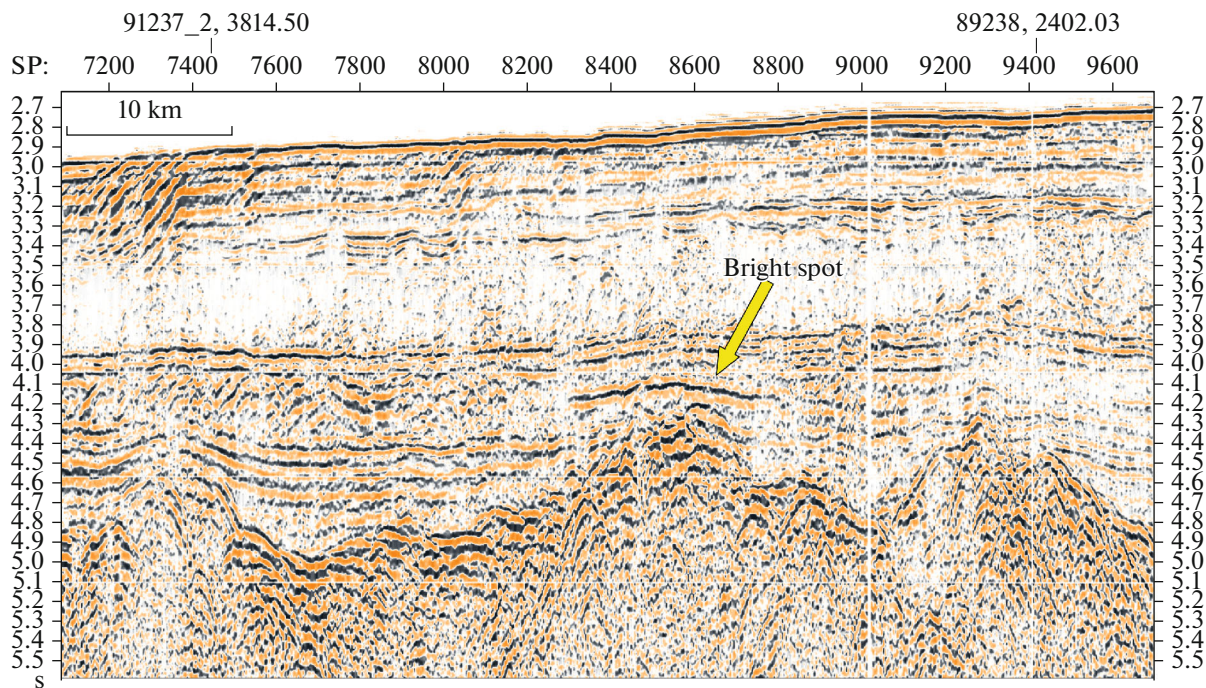
sively in the upper part of the sedimentary section based on these data. The allocated spots were checked for fluid pools by calculating the seismic attribute of the instantaneous frequency in the RadExPro package. Local minimums of the attribute along the reflectors indicate a local decrease in layer velocities due to fluid saturation. The results of picking were exported to the ArcGIS cartographic environment, where, first of all, the cartographic position of spots was shown on a topographic basis of geophysical fields. In addition, the spots were assigned the values of these fields corresponding to their centers, which showed that the spatial position of spots was confined to certain zones in the basement of the eastern flank of the Knipovich Ridge.

#### RESULTS AND PRIMARY INTERPRETATION

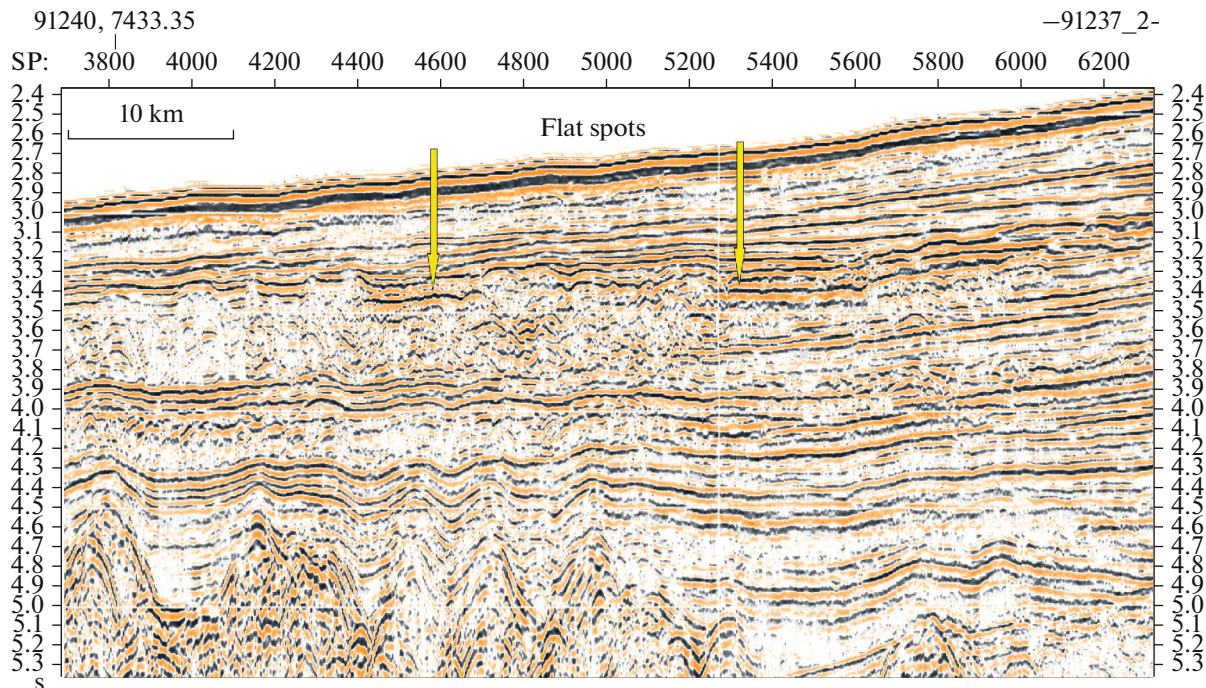
Interpretation of the seismic data made it possible to identify 24 anomalies of the wave field referred to the “bright” or “flat” spots. Figures 4–7 present examples of these anomalies.

Figure 6 shows a fragment of the CSP section S26-52 with a fluid anomaly of the bright spot type (thickness ~160 ms (~120 m), horizontal size 12 km). Given that the horizontal dimensions are isometric, the pool volume will be 13.5 bln m<sup>3</sup>. The anomaly fills an anti-form overlain by similar reflector configuration that does not yield an anomalous record, suggesting a local rise of unconsolidated sediments under fluid pressure or deformation of sediments during the vertical movement of basement blocks. There is another smaller spot west of the big spot. Section S24-P2-12b (Fig. 7) extending from the Hovgaard Ridge to the western wall of the Knipovich Ridge is equipped with a fragment of the seismic record with the bright spot-type fluid anomaly located above the BSR gap. Thickness of the anomaly is ~120 ms (~90 m), and the horizontal size is 4 km. The anomaly fills the anti-form overlain by a conformal deformation of the bottom profile, probably, also suggesting a local rise of unconsolidated sediments under the pressure of fluids migrated upward the section through the fracture in the fluid-confining rocks.

The sublatitudinal sections including the seismic record anomalies and acoustic basement shows the deformations of preglacial and, in some cases, glacial sedimentary sequences, which can be deformed by vertical movements of the consolidated crust blocks. Deformations of the sedimentary cover above the basement are minimal at the sublongitudinal section 91240 (Fig. 1), which also indicates the sublongitudinal orientation of the folded front axis. The spatial position of anomalies is shown in Fig. 8 based on the residual Bouguer anomaly as a topographic basis. In this paper, residual anomalies are understood as a high-frequency component of the field with the wavelength less than 65 km. This value of the boundary frequency was chosen in order to ensure the effect of den-



**Fig. 4.** Fragment of the CDP-SRM section 91240 (the position is shown in Fig. 1) including the seismic anomaly of the bright spot type above the acoustic basement projection. Horizontal axis shows the stacked trace number.



**Fig. 5.** Fragment of the CDP-SRM section 91237\_2 (the position is shown in Fig. 1) including the seismic anomaly of the “flat spot” type above the ledge of the acoustic basement. Horizontal axis shows the stacked trace number.

sity inhomogeneities (after filtration of the field transformant) in the serpentinization-prone crust and upper mantle.

The field of Bouguer residual anomalies (Fig. 8) shows that the linear structure associated with the Senja fracture zone continues to the NNW. This con-

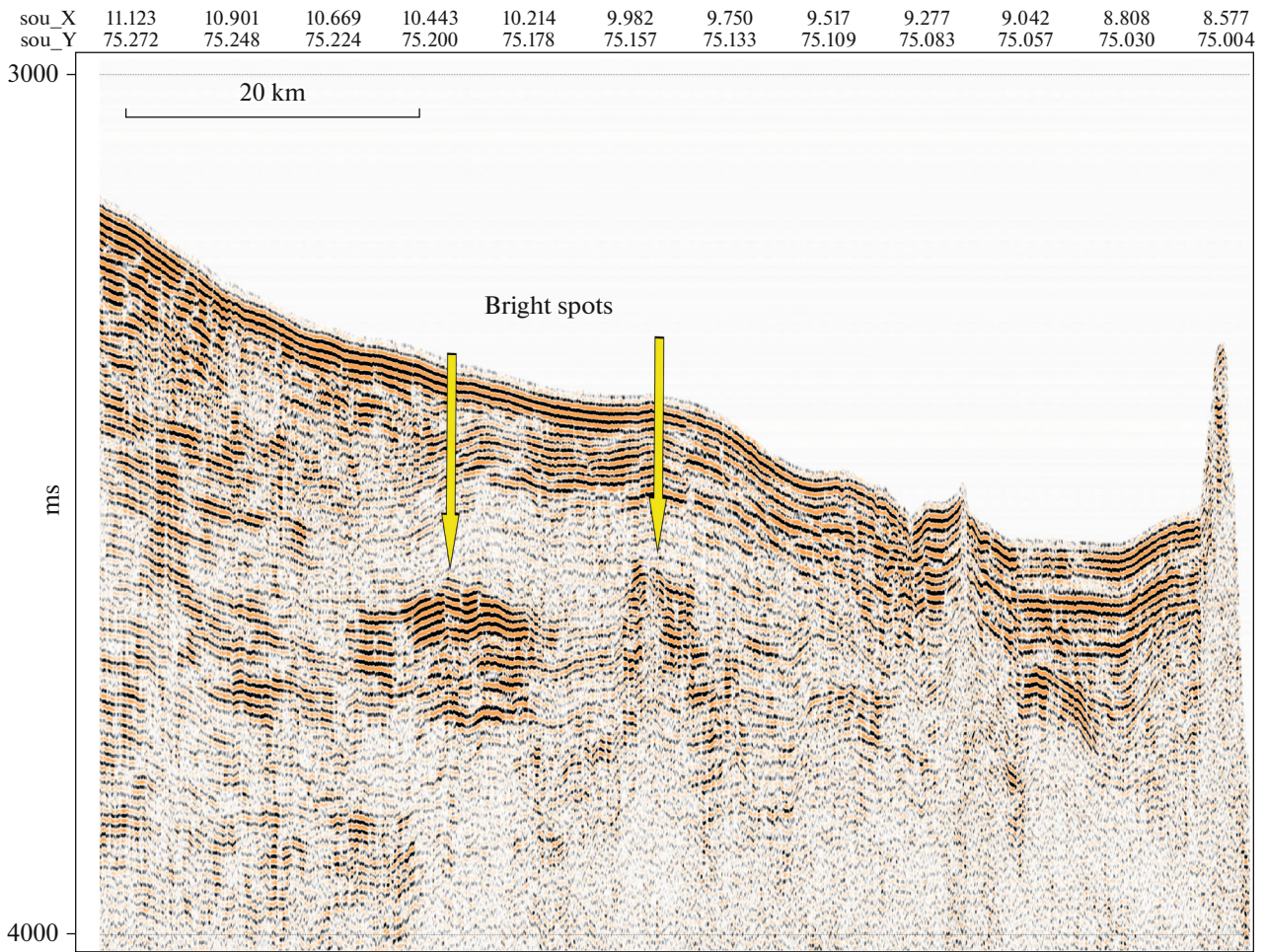


**Fig. 6.** A fragment of the CSP section S26-52 including seismic anomaly record of the bright spot type above the projections of the acoustic basement. Horizontal axis shows the longitude and latitude (decimal degrees).

sou_X	3.019	3.192	3.367	3.544	3.725	3.912	4.099	4.284	4.467	4.650	4.834	5.017	5.201	5.384	5.569	5.756	5.943	6.131
sou_Y	78.342	78.345	78.347	78.349	78.351	78.353	78.355	78.357	78.359	78.360	78.362	78.363	78.365	78.366	78.367	78.368	78.368	78.369

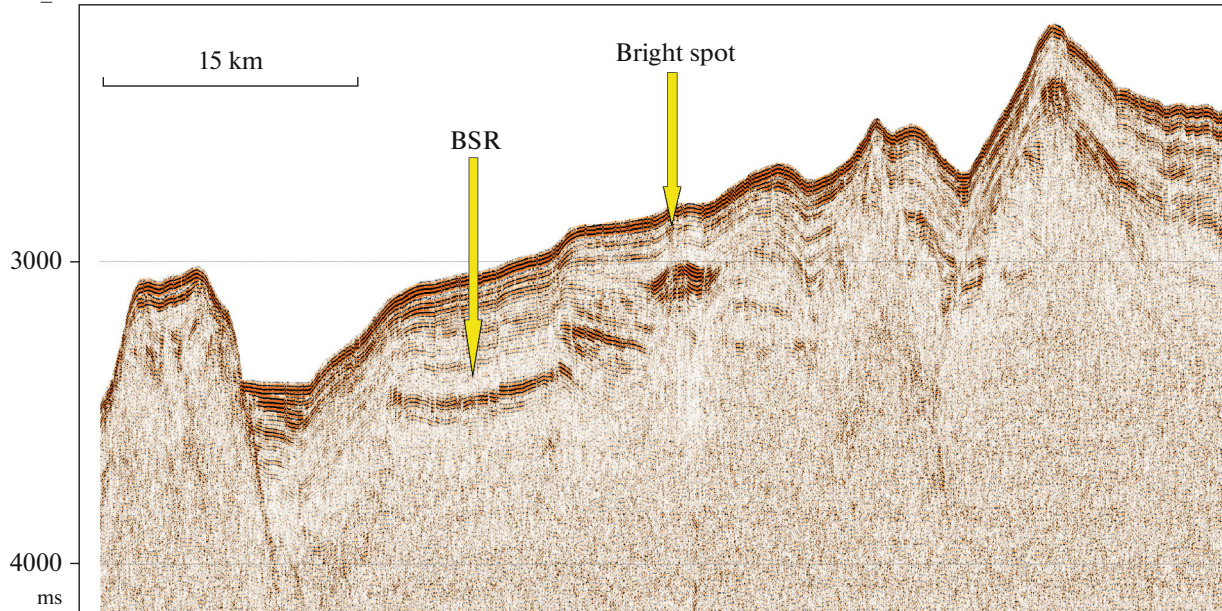


**Fig. 7.** Fragment of the CSP section S26-P2-12b including anomalies of the bright spot type seismic record and BSR anomalies. Horizontal axis shows the longitude and latitude (decimal degrees).

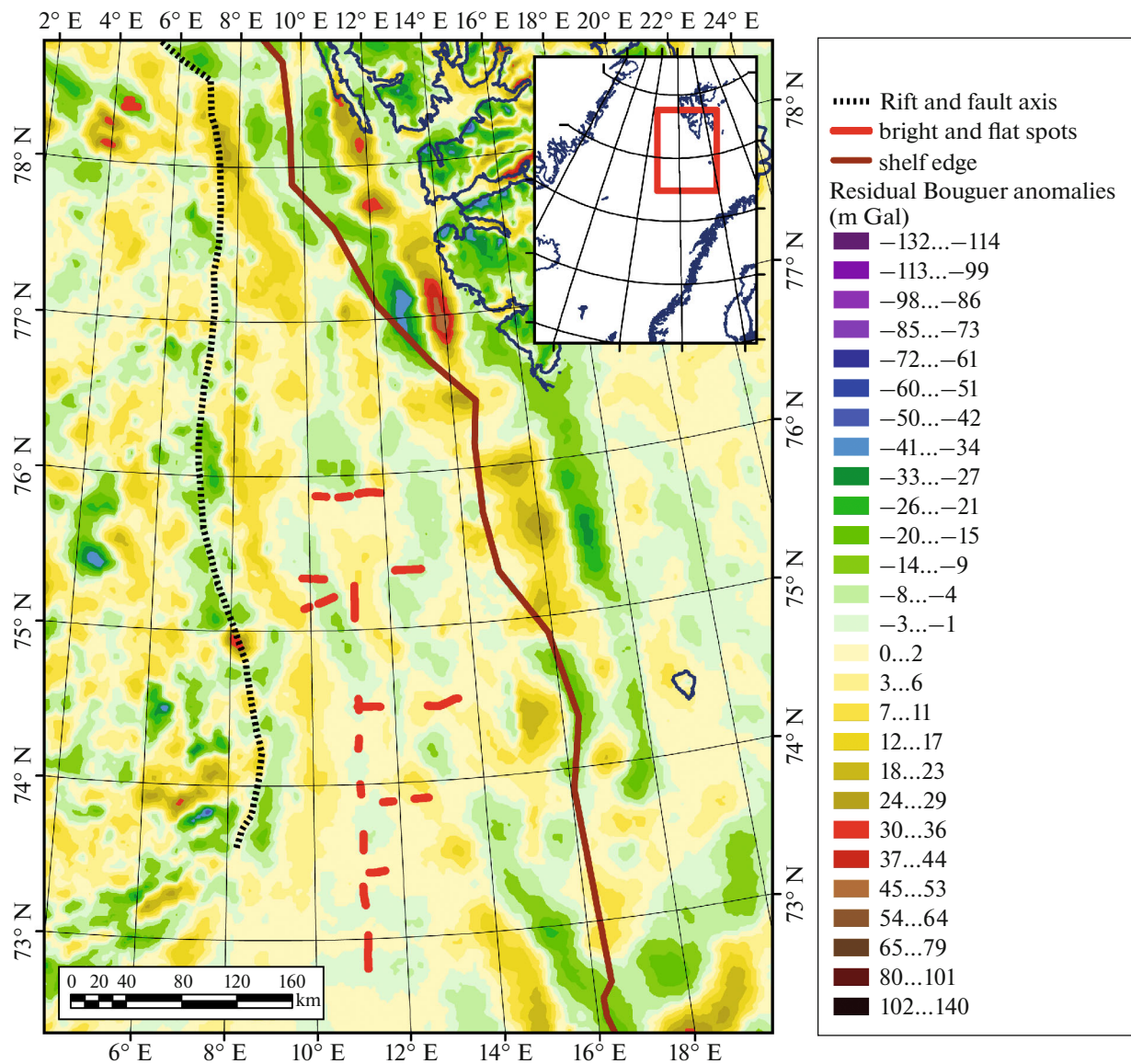


**Fig. 8.** Position of seismic anomalies of the bright and flat spot types, based on the topobasis of the residual Bouguer anomaly yielded by the high-frequency filtration of the full Bouguer anomaly for wavelengths  $\leq 65$  km.

tinuation represents a linear maximum–minimum pair sticking into the Knipovich Ridge near 76° N. The location of most spots is associated with negative zones of residual anomaly. The particularly deep minimum of the field is associated with a few anomalies north of 78° N. Average value in the area of anomalies on both walls of the Ridge is close to zero after filtration (0.3 mGal), the average value is  $-2.7$  mGal beneath the anomalies and  $-0.5$  mGal on the southeastern flank of the ridge. Comparison of the spatial position of the anomalies with the anomalous magnetic field  $\Delta T_a$ , according to (Olesen et al., 1997) (Fig. 9), shows that the anomalies are confined mainly to mosaic areas of the field marked by the lack of linear configuration. In addition, average level of the mag-

netic field in the seismic anomalies is  $+72$  nT and almost all seismic anomalies lie within the limits of significant positive magnetic anomalies.

#### DISCUSSION AND GEODYNAMIC INTERPRETATION

The obtained results show that continuation of the ocean–continent transform boundary along the Senja fracture zone is marked by the tectonic reactivation manifested by the following unique configuration of earthquake epicenters (Fig. 3). Events on the eastern flank of the Knipovich Ridge are arranged as long chains along the fracture zone continuation and as orthogonal short chains with numerous weak events.

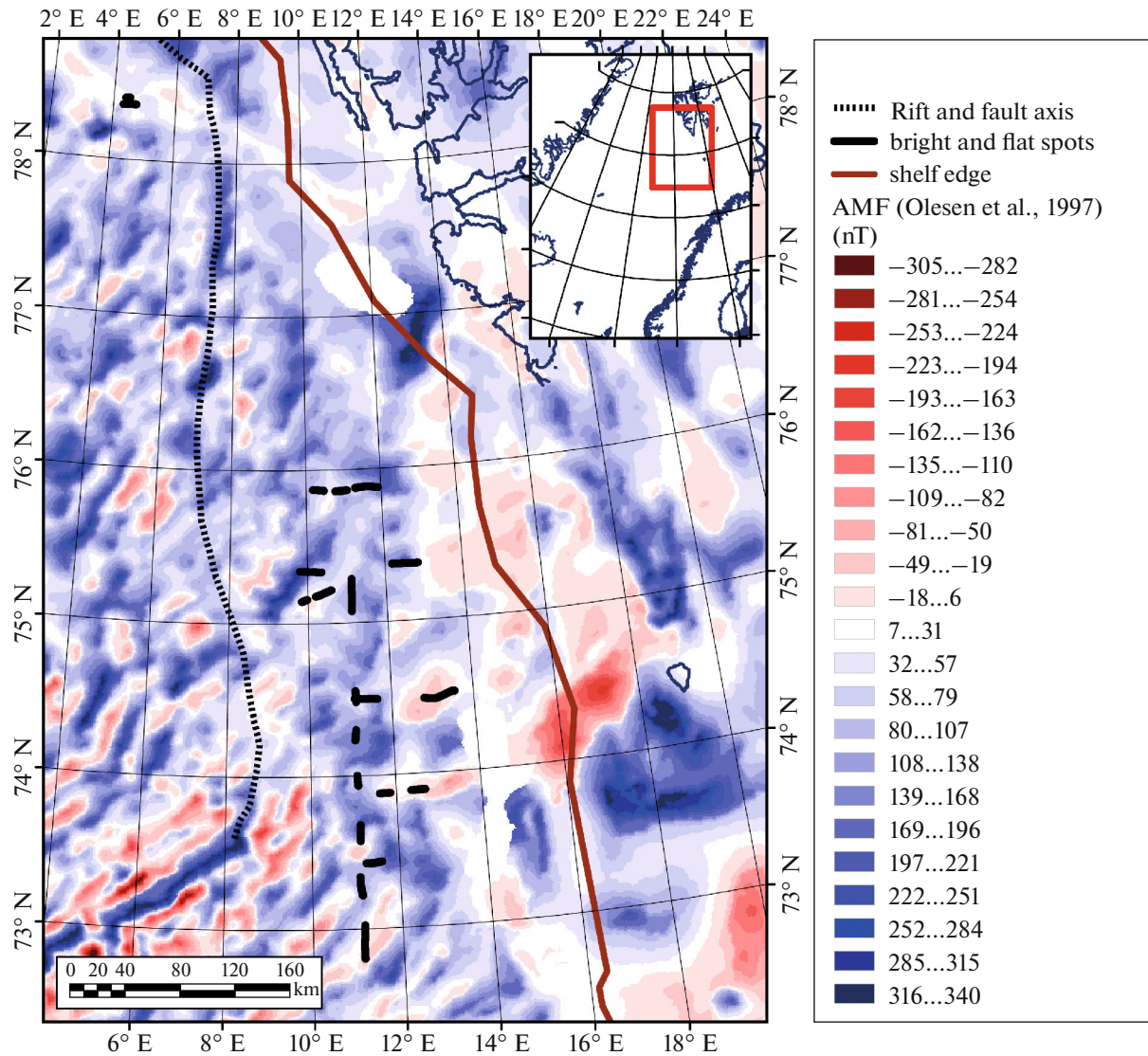


**Fig. 9.** Position of seismic anomalies of the bright and flat spot types based on the topobasis of the anomalous magnetic field  $\Delta T_a$  data, according to (Olesen et al., 1997).

Such spatial distribution of seismic events mimics the classical distribution along the standard structural elements of a divergent boundary (rift segments and transform faults) but with a  $\sim 60^\circ$  orientation relative to the modern ridge. The orientation of these epicenters also does not coincide with the orientation of linear magnetic anomalies in those places where they are detected as short segments (Fig. 9), suggesting that the active basement structures are superimposed on the primary structure. Long chains of events on the flank are located along the elongated residual Bouguer anomalies (Fig. 8), which is a continuation of the Senja fracture zone. Hence, the basement structures making up variations of residual Bouguer anomalies are experiencing modern alternating movements. The rise of consolidated crust blocks provokes deformations in the sedimentary cover (Figs. 4, 5). According

to (Kandilarov et al., 2008; Rajan et al., 2012), the downwarping of blocks is related to the detachment on the eastern flank of the Knipovich Ridge. According to (Rajan et al., 2012), detachment on the Knipovich Ridge and its flanks is accompanied by serpentinization in the upper mantle and is exemplified by a seismic section with a “flat spot” anomaly. Serpentinization is accompanied by decompaction, dilatation, and gas generation, leading to positive vertical movements and gas accumulation in the sediments overlying the basement.

In areas with the most intense degassing (Fig. 7) in deep zones of the Svyatogor Rise, the upward migrated gas forms a gas hydrate layer with the BSR bottom (Waghorn et al., 2018), which serves as a fluid-confining barrier for the rising fluid flow. If the BSR integrity is distorted, the fluid flow makes up heave mounds in

weakly consolidated sediments (Figs. 6, 7). Based on the CDP-SRM data, many bright spot anomalies in the preglacial sedimentary sequence are located above the acoustic basement highs in accordance with the hypothesis of link with serpentinization. The average residual Bouguer anomaly beneath seismic anomalies is at least 1 to 3 mGal lower than the total average value of this transformant near zero. This fact indicates the presence of crust and/or upper mantle decompaction zones associated with serpentinization. Average value of the anomalous magnetic field at seismic anomalies is +72 nT and is almost entirely in the positive range, regardless of the distance to the ridge, and, consequently, of age. Hence, serpentinization, accompanied by the formation of magnetite, can be a modern coeval regional process producing the superimposed chemogenic magnetoactive layer in the upper mantle. This scenario can explain the mosaic pattern of the anomalous magnetic field and the loss of correlability of classical spreading magnetic linear anomalies typical for flanks of the Knipovich Ridge (Olesen et al., 1997).

## CONCLUSIONS

1. The eastern flank of the Knipovich Ridge is undergoing tectonic reactivation along the basement of structures that make up the northern continuation of the Senja fracture zone and are inconsistent with the orientation of both rift segments of the ridge and transform displacements therein. These structures are expressed in the high-frequency component of Bouguer anomalies and are accompanied by deformations of the sedimentary cover above the basement, according to the seismic data.

2. Anomalies of the bright or flat spot type identified from the seismic data are related to the process of degassing. Such anomalies are located in areas with negative values of the residual Bouguer anomaly and positive anomalies of the magnetic field, suggesting correlation of anomalies with decompaction zones, probably, associated with serpentinization accompanied by the formation of methane and the superimposed chemogenic magnetization, which distorts the primary linear pattern of magnetic anomalies from the spreading basement. The positive value of the anomalous magnetic field indicates the modern age of these processes.

3. Vertical displacements of the crustal and upper mantle blocks on flanks leading to deformations of the sedimentary cover and off-axis seismicity can be explained by rock dilatation as a result of serpentinization and tectonic detachments on the flanks. The consequent increase in the access of water needed for this process changed the physical properties of rocks (sources of geophysical fields).

## ACKNOWLEDGMENTS

The authors express gratitude to Russian Federal Geological Fund (<https://rfgf.ru>) for access to unpublished materials needed for the research and to Marine Arctic Geological Expedition for the CDP-SRM digital data. The authors are also grateful to two anonymous reviewers whose comments helped to improve the text and graphic materials in the paper.

## FUNDING

This work was supported by State Tasks of the Geological Institute, Russian Academy of Sciences. The primary processing of seismic data was financed by the Russian Foundation of Basic Research project no. 18-05-70040.

## REFERENCES

- Amundsen, I., Blinova, M., Hjelstuen, B., Mjelde, R., and Haflidason, H., The Cenozoic western Svalbard margin: sediment geometry and sedimentary processes in an area of ultraslow oceanic spreading, *Mar. Geophys. Res.*, 2011, vol. 32, pp. 441–453.
- Balmino, G., Vales, N., Bonvalot, S., and Briais, A., Spherical harmonic modeling to ultra-high degree of Bouguer and isostatic anomalies, *J. Geod.*, 2012, vol. 86, pp. 499–520.
- Baturin, D.G., Structure of the sedimentary cover and development of the Spitsbergen continental margin, in *Osa-dochnyi chekhol Zapadno-Arkticheskoi metaplatforny* (Sedimentary Cover of the West Arctic Megaplatform), Murmansk, 1993, pp. 35–47.
- Bougault, H., Hydrogène et méthane hydrothermal: Enjeux scientifiques une ressource potentielle nouvelle?, *Mines Carr. Industr. Miner.*, 2012, no. 196, pp. 73–80.
- Chamov, N.P., Sokolov, S.Yu., Kostyleva, V.V., Efimov, V.N., Peive, A.A., Aleksandrova, G.N., Bylinskaya, M.E., Radionova, E.P., and Stupin, S.I., Structure and composition of the sedimentary cover in the Knipovich Rift Valley and Molloy Deep (Norwegian–Greenland Basin), *Lithol. Miner. Resour.*, 2010, no. 6, pp. 532–554.
- Charlou, J.L., Fouquet, Y., Bougault, H., Donval, J.P., Etoubleau, J., Jean-Baptiste, P., Dapoigny, A., Appriou, P., and Rona, P., Intense CH<sub>4</sub> plumes generated by serpentinization of ultramafic rocks at the intersection of the 15°20' N fracture zone and the Mid-Atlantic Ridge, *Geochim. Cosmochim. Acta*, 1998, vol. 62, no. 13, pp. 2323–2333.
- Cherkashev, G.A., Gusev, E.A., Zhirnov, E.A., Tamaki, K., Kurevits, D., Okino, K., Sato, H., Baranov, B.V., Egorov, A.V., German, K., Crane, K., and Sushchevskaya, N.M., The Knipovich Ridge Rift Zone: Evidence from the Knipovich-2000 expedition, *Dokl. Earth Sci.*, 2001, vol. 378, pp. 420–423.
- Delescluse, M. and Chamot-Rooke, N., Serpentinization pulse in the actively deforming Central Indian Basin, *Earth Planet. Sci. Lett.*, 2008, vol. 276, pp. 140–151.
- Dmitriev, L.V., Bazylev, B.A., Silantiev, S.A., Borisov, M.V., Sokolov, S.Yu., and Bougault, H., Hydrogen and methane formation with serpentinization of mantle hyperbasite of the ocean and oil generation, *Russ. J. Earth Sci.*, 1999, vol. 1, no. 6, pp. 511–519.

- Fizicheskie svoystva gornyykh porod i poleznykh iskopaemykh (petrofizika). Spravochnik geofizika (Physical Properties of Rocks and Useful Minerals— Petrophysics): A Manual for Physicists*, Dortman, N.B., Ed., Moscow: Nedra, 1984.
- Gernigon, L., Franke, D., Geoffroy, L., Schiffer, C., Foulger, G.R., and Stoker, M., Crustal fragmentation, magmatism, and the diachronous opening of the Norwegian-Greenland Sea, *Earth-Sci. Rev.*, 2020, vol. 206, pp. 1–37.
- Johnson, J.E., Mienert, J., Plaza-Faverola, A., Vadakkepuliambatta, S., Knies, J., Bünz S., Andreassen K., and Ferré B., Abiotic methane from ultraslow-spreading ridges can charge Arctic gas hydrates, *Geology*, 2015, vol. 43, no. 5, pp. 371–374.
- Kandilarov, Ferre, B., Abiotic methane from ultraslow-spreading ridges can charge Arctic gas hydrates, A., Mjelde, R., Okino, K., and Murai, Y., Crustal structure of the ultraslow spreading Knipovich Ridge, North Atlantic, along a presumed amagmatic portion of oceanic crustal formation, *Mar. Geophys. Res.*, 2008, vol. 29, pp. 109–134.
- Kandilarov, A., Landa, H., Mjelde, R., Pedersen, R.B., Okino, K., and Murai, Y., Crustal structure of the ultraslow spreading Knipovich Ridge, North Atlantic, along a presumed ridge segment center, *Mar. Geophys. Res.*, 2010, vol. 31, pp. 173–195.
- Keir, R.S., Greinert, J., Rhein, M., and Petrick, G., Sültenfuß, J., and Fürhaupter, K., Methane and methane carbon isotope ratios in the Northeast Atlantic including the Mid-Atlantic Ridge (50° N), *Deep-Sea Res. I*, 2005, vol. 52, pp. 1043–1070.
- Kvarven, T., Hjelstuen, B., and Mjelde, R., Tectonic and sedimentary processes along the ultraslow Knipovich spreading ridge, *Mar. Geophys. Res.*, 2014, vol. 35, pp. 89–103.
- Maus, S., Barckhausen, U., Berkenbosch, H., Bournas, N., Brozena, J., Childers, V., Dostaler, F., Fairhead, J.D., Finn, C., von Frese, R.R.B., Gaina, C., Golynsky, S., Kucks, R., Luhr, H., Milligan, P., Mogren, S., Müller, R.D., Olesen, O., Pilkington, M., Saltus, R., Schreckenberger, B., Thebault, E., and Tontini, F.C., EMAG2: A 2-arc-minute resolution Earth Magnetic Anomaly Grid compiled from satellite, airborne and marine magnetic measurements, *Geochem. Geophys. Geosyst.*, 2009, vol. 10, no. 8, pp. 1–12.
- Mosar, J., Eide, E.A., and Osmundsen, P., et al., Greenland-Norway separation. A geodynamic model for the North Atlantic, *Norw. J. Geol.*, 2002, vol. 82, pp. 281–298.
- NORSAR Reviewed Regional Seismic Bulletin*. 2012. Available from <http://www.norsardata.no/NDC/bulletins/regional/>.
- Olesen, O.G., Gellein, J., Habrekke, H., et al., *Magnetic Anomaly Map, Norway and Adjacent Ocean Areas*, Scale 1:3 Million, *Geol. Surv. Norway*, 1997.
- Plaza-Faverola, A. and Keiding, M., Correlation between tectonic stress regimes and methane seepage on the western Svalbard margin, *Solid Earth*, 2019, vol. 10, pp. 79–94.
- Rajan, A., Mienert, J., Bunz, S., and Chand, S., Potential serpentinization, degassing, and gas hydrate formation at a young (<20 Ma) sedimented ocean crust of the Arctic Ocean ridge system, *J. Geophys. Res.*, 2012, vol. 117, p. B03102.
- Rebesco, M., Wahlin, A., Laberg, J.S., et al., Quaternary contourite drifts of the Western Spitsbergen margin, *Deep-Sea Res. I*, 2013, vol. 79, pp. 156–168.
- Rebesco, M., Hernández -Molina, F.J., Van Rooij, D., and Wahlin, A., Contourites and associated sediments controlled by deep-water circulation processes: State-of-the-art and future considerations, *Mar. Geol.*, 2014, vol. 352, pp. 111–154.
- Peive, A.A. and Chamov, N.P., Basic tectonic features of the Knipovich Ridge (North Atlantic) and its Neotectonic evolution, *Geotectonics*, 2008, no. 1, pp. 31–47.
- Sokolov, S.Yu., Tectonic evolution of the Knipovich Ridge based on the anomalous magnetic field, *Dokl. Earth Sci.*, 2011, vol. 437, no. 3, pp. 343–348.
- Sokolov, S.Yu., Abramova, A.S., Moroz, E.A., and Zaiskaya, Yu.A., Amplitudes of fractures on flanks of the Knipovich Ridge (North Atlantic): Indicator of modern regional geodynamics, *Geodinam. Tektonofiz.*, 2017, vol. 8, no. 4, pp. 769–789.
- Shipilov, E.V., Shkarubo, S.I., and Raznitsin, Yu.N., Neotectonics of the northern Norwegian–Greenland Basin: Specific features and evolution of the Knipovich Ridge and Pomorsky perioceanic trough, *Dokl. Earth Sci.*, 2006, vol. 410, no. 4, pp. 1056–1061.
- Shkarubo, S.I., Specific features of spreading in the northern Norwegian–Greenland Basin, in *Geologo-geofizicheskie kharakteristiki litosfery Arkticheskogo regiona (Geological-Geophysical Characteristics of the Arctic Lithosphere)*, St. Petersburg: VNIIOkeangeologiya, 1996, pp. 101–114.
- Yampol'skiy, K.P. and Sokolov, S.Yu., Sedimentary cover and Bouguer anomalies in the northern part of the Knipovich Ridge, *Dokl. Earth Sci.*, 2012, vol. 442, no. 4, pp. 188–192.
- Straume, E.O., Gaina, C., Medvedev, S., Hochmuth, K., Gohl, K., Whittaker, J.M., et al., GlobseD: updated total sediment thickness in the world's oceans, *Geochem. Geophys. Geosyst.*, 2019, vol. 20, pp. 1756–1772.
- Waghorn, K.A., Bünz, S., Plaza-Faverola, A., and Johnson, J.E., 3D seismic investigation of a gas hydrate and fluid flow system on an active mid-ocean ridge; Svyatogor Ridge, Fram Strait, *Geochem. Geophys. Geosyst.*, 2018, vol. 19, pp. 2325–2341.
- Zaionchek, A.V., Brekke, Kh., Sokolov, S.Yu., Mazarovich, A.O., Dobrolyubova, K.O., Efimov, V.N., Abramova, A.S., Zaiskaya, Yu.A., Kokhan, A.V., Moroz, E.A., Peive, A.A., Chamov, N.P., and Yampol'skii, K.P., Structure of the continent-ocean transition zone in the north-western framing of the Barentsmoray Sea (based on the data from cruises 24, 25, and 26 of the R/V Akademik Nikolaj Strakhov (2006–2009)), in *Stroenie i istoriya razvitiya litosfery (Structure and History of the Lithosphere Development)*, Moscow: Paulsen, 2010, vol. 4, pp. 111–157.

Translated by D. Sakya